Catalysis Today 137 (2008) 71–79

Contents lists available at ScienceDirect

Catalysis Today

journal homepage: www.elsevier.com/locate/cattod

Deactivation handling in a high-throughput kinetic study of *o*-xylene hydrogenation

G. Morra [c], D. Farrusseng [a,*], E. Guillon [b], S. Morin [b], C. Bouchy [b], P. Duchêne [b], C. Mirodatos [a]

[a] IRCELYON, Institut de recherches sur la catalyse et l'environnement de Lyon, 2 avenue Albert Einstein, Villeurbanne, F-69626 cedex, CNRS, UMR5256, France
[b] IFP-Lyon, BP 3, 69360 Solaize, France
[c] Johnson-Matthey Catalysts, PO Box 1, Belasis Avenue, Billingham, TS23 1LB, United-Kingdom

ARTICLE INFO

Article history:
Available online 21 May 2008

Keywords:
High-throughput experimentation
Combinatorial catalysis
Deactivation
Kinetic modeling
Xylene hydrogenation
Kinetic descriptors

ABSTRACT

The objective of the study is to develop an HT methodology to enable kinetic modeling of diverse catalysts. The reaction of *o*-xylene hydrogenation is selected as a probe reaction to evaluate the "metallic" features of a library of about 80 diverse bimetallic catalysts. A major issue to overcome is deactivation phenomena which are catalyst dependent and which cannot *a priori* be predicted. A prerequisite is therefore to handle correctly deactivation processes for accessing intrinsic kinetic parameters. For this purpose, an adapted screening strategy is developed, using a proprietary 16 channels multi-tubular reactor which enables to test catalysts at the same time-on-stream. Original data treatment procedures are implemented in order to correct observed data from deactivation phenomena for the calculation of kinetic parameters. Effects of metal nature, dopants and supports on deactivation rate are analyzed using a statistical approach, and a tentative classification of deactivation processes based on coke analyses performed on aged materials is provided.

1. Introduction

In contrast to a primary catalyst screening that aims to discover hits, the purpose of testing catalysts in parallel manner against a model reaction is to get rapid access to quantitative information describing some catalyst features. In that respect, kinetic modeling is an appropriate mean to describe catalyst profiles in a quantitative manner.

Within the frame of refinery chemistry, benzene, toluene and xylenes are model molecules frequently used for investigating the key process of aromatic hydrocarbons hydrogenation. For these model reactions, a number of kinetic models were developed from simple power laws to detailed micro-kinetic models [1–4]. Despite the relative simplicity of these model reactions (toluene and xylenes hydrogenation), there is no general agreement on a mechanism (e.g., rate determining hydrogenation step for toluene [5], xylene [2], roll-over vs. interfacial sites [3], etc.). As a result, many different macro- and micro-kinetic models were developed. It may come from differences in reaction conditions and kinetic approaches but also from differences in catalytic systems (e.g., Ni [6], Pt [7], zeolite [8]). Indeed, a kinetic model is usually supported by experimental data acquired with a specific class of catalysts. Hence the extrapolation to other catalytic formulation is always questionable. A kinetic model holding for diverse catalysts, e.g., different metallic sites, dopants and supports would enable to describe and compare in a quantitative manner diverse catalysts by the direct comparison of their respective kinetic parameters.

In addition to different catalyst formulation, a second major issue to be tackled for any kinetic study is deactivation phenomena (carbon deposits, particle growth, metal/support interaction, alloy formation or demixing, poisoning, etc.) which are specific of each catalyst and cannot *a priori* be predicted. This issue may be even more critical during high-throughput (HT) parallel investigation since when a catalyst is under testing, deactivation of other catalysts is not monitored. Selecting only catalysts that do not deactivate with time on stream for parallel screening would strongly limit the diversity of the investigated libraries, which cannot be envisaged for industrial oriented projects [9]. The investigation of aging kinetics is therefore a prerequisite for handling properly reaction kinetics [10–12].

This work deals with the development of a relevant methodology which aims at accelerating kinetic modeling on diverse catalyst libraries by means of HT experimentation. The screening of about 80 bimetallic catalysts is carried out on a 16-parallel channel reactor enabling to test catalysts under identical time-on-stream conditions [13]. A robust kinetic model, which can accommodate diverse catalytic behaviors, is developed for the *o*-xylene hydrogenation, using a benchmark catalyst. Deactivation profiles are

* Corresponding author. Tel.: +33 04 72 44 53 65.
E-mail address: david.farrusseng@ircelyon.univ-lyon1.fr (D. Farrusseng).

0920-5861/$ – see front matter © 2008 Elsevier B.V. All rights reserved.
doi:10.1016/j.cattod.2008.03.025

modeled and various mechanisms are discussed. From the observed impact of deactivation on kinetic parameters, a method which enables to correct kinetic parameters from deactivation is described. Finally, relationships between catalyst composition and deactivation features are highlighted and discussed.

2. Experimental

2.1. Parallel reactor for HT screening

A proprietary 16 channel-multi-tubular reactor which is now commercialized as the SWITCH 16 reactor system by AMTEC GmbH [14], was adapted for the *o*-xylene hydrogenation reaction. The fluidic supply consists of a combination of two separate feed delivery modules and two 16-port valves which are placed before and after the multi-channel reactor array. This system offers the opportunity to feed one selected reactor with a selected feed composition (feed 1) while the 15 others are fed with a second composition (feed 2), which can be identical to or different from feed 1. This design has several advantages regarding testing capabilities and the type of experiments which can be carried out, i.e., it is possible to evaluate catalysts under exactly the same ageing period and more specifically to measure the initial activity of each catalyst. Testing conditions can be varied in the selected channel while the other channels are maintained under standard or inert conditions. In addition, catalyst deactivation can be studied in the selected channel while the 15 other channels are being regenerated. Finally, this design, ensures very accurate and reproducible flows in the selected channel by the 16-port valve.

Mixtures of *o*-xylene (Fluka, *purissim p.a.*, ≥99%) and heptane (Riedel-De Haen, *purissim p.a.*, ≥99%) used as diluent (1:9 wt ratio) were supplied by a syringe delivery system. The *o*-xylene contains less than 0.5%. of *cis*- and *trans*-1,2-dimethylcyclohexane (DMCH) as impurities.

Gas chromatography (GC) analysis was performed by using an Agilent 3000 version QUAD instrument equipped with a four-channel module. Channel A was used for H_2, N_2, measurements (MolSieve 5A, BF PPU Plot, with Ar as carrier gas). Channel C for *cis*- and *trans*-dimethyl-cyclohexane (OV1) and Channel D for *o*-xylene quantification (Stabilwax). Each GC analysis was duplicated.

2.2. Catalyst library

A combinatorial library of 80 supported bimetallic samples was prepared, on the basis of known or foreseen diversity of catalytic behaviors). Preliminary results on 44 catalysts are presented in this study. Examples of catalysts are provided in Table 1. Catalysts were made by combining a main hydrogenating metal among Rh, Pt, Pd and Ni and a secondary element as additive among six possibilities (Mo, Mn, Sn and three other undisclosed elements). The catalysts were prepared by incipient wetness impregnation starting from chlorine free precursors to yield about 4 g of dried powder. Successive impregnations of different precursors were carried out when precursors were not miscible. The solids were calcined at 450 °C in N_2 flow for 1 h. The amount of secondary element can take two levels (high or low corresponding to element II/element I molar ratio = 2.64 and 0.66, respectively). Two sieved supports (250–360 μm) were investigated with low and high surface area, respectively αθ- and γ-alumina.

2.3. Testing methodology

The catalysts were tested sequentially, following a three-step procedure, which allows us to study the kinetics of a selected catalyst for a few hours while other catalysts are maintained under H_2/N_2 flow. The switching protocol described in Section 2 was used for this purpose.

Table 1
Example of catalysts with diverse formulation, initial activity and deactivation profile in *o*-xylene hydrogenation

#	Metal load	Support	Mass (mg)
1	4% Ni–0.16% Mo	αθ-Al_2O_3	50
2	4% Ni–0.44% Mn	γ-Al_2O_3	30
3	4% Ni	γ-Al_2O_3	200
4	0.5% Pt–0.16% Mo	γ-Al_2O_3	30
5	0.5% Pt–0.2% Sn	αθ-Al_2O_3	30
6	0.5% Pt–0.8% Sn	γ-Al_2O_3	200
7 (benchmark)	0.3 Pd	αθ-Al_2O_3	200

Catalyst #7 was characterized and tested in details and is used as a benchmark.

(i) Step I consists at recording the initial activity for 1 h at constant conditions of temperature and partial pressures.
(ii) Then, in step II, kinetic data are obtained by varying H_2 partial pressure at a given temperature. The process is repeated at different temperature from 100 °C to 200 °C.
(iii) Finally, in step III, when the whole set of experimental conditions is completed for kinetic studies, the initial conditions (step I) are restored in order to estimate the deactivation which has occurred during the kinetic step II.

When the three steps are completed, the selection valve switches to the next catalyst and the procedure is repeated.

2.4. Testing conditions

Generally speaking, it was observed that under the same operating conditions, conversion can attain the thermodynamic equilibrium for a given catalyst but remain below detection limits for another catalyst with a different dopant. This parameter sensitivity causes experimental issues when one wants to investigate kinetics. As a consequence, the catalyst mass in the channel, i.e., contact time, must be adjusted with respect to its activity level in order to measure conversions in appropriate ranges for further kinetic modeling (outside diffusion regime but being large enough for accurate measurements). From these statements, the following testing conditions were applied: (i) all catalysts are previously reduced in situ under H_2 at 400 °C for 2 h, (ii) for the initial deactivation study, catalysts are tested with a stream of 0.5 mol.% *o*-xylene, 5 mol.% heptane, 25 mol.% hydrogen and nitrogen as diluent (Feed 2). The other channels are maintained under H_2/N_2 flow (Feed 1), (iii) for the kinetic study, reactors are loaded with 50 mg, 100 mg, 200 mg or 400 mg of catalysts depending on their conversion level and SiC completion maintained catalyst volume at 0.23 cm^3. The H_2 partial pressure was varied from 10 mol.% to 85 mol.%, the temperature from 100 °C and 200 °C and the total flow was maintained constant at 1 L_{STP}/h. (STP: 1 atm, 0 °C) The weight hourly space velocities (catalyst weight/hydrocarbon flow) were kept between 1.1 h and 9 h.

2.5. Kinetic modeling

In order to test different kinetic models, a catalyst (catalyst #7) which does not deactivate under the experimental conditions was selected as reference material. A large dataset of more than 200 data points was collected and used as benchmark for model discrimination and to simulate the impact of deactivation rates on the kinetic parameters.

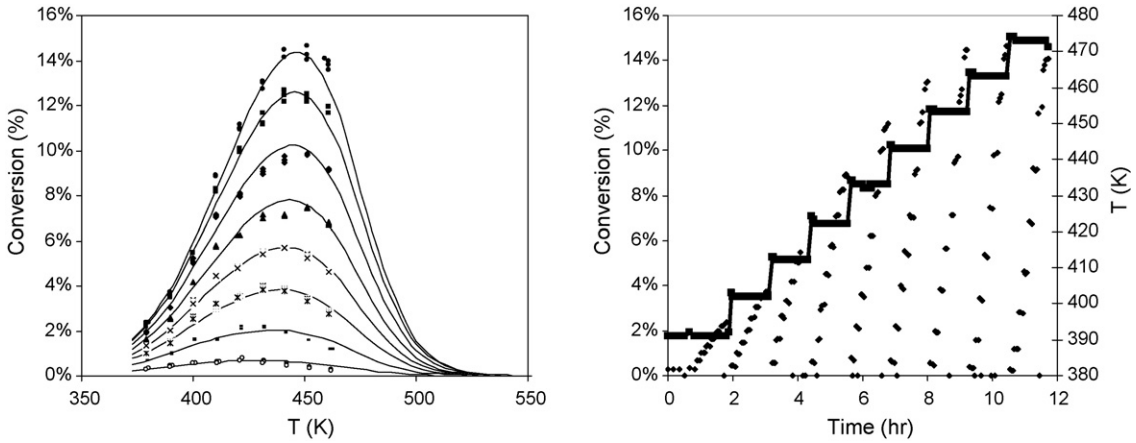

Fig. 1. Catalyst #7 kinetic data. (Left) Conversion profiles as a function of H_2 partial pressure and temperature. *Dots*: experimental points with H_2 partial pressure serials: (○) 0.1 bar, (−) 0.22 bar, (*) 0.33 bar, (×) 0.44 bar, (▲) 0.56 bar, (◆) 0.68 bar, (■) 0.79 bar, (●) 0.85 bar; *line*: corresponding simulation. (Right) Mapping of kinetic data acquisition as a function of time on stream and temperature. *Dots*: conversion (%); *line*: temperature (K).

Fig. 1(left) shows experimental conversion data and the results of the kinetic modeling. The order of data acquisition is reported in Fig. 1(right) as a function of time. We can observe that the conversion depends very much on the H_2 partial pressure at a given temperature.

Different kinetic models and variations of thereof were investigated, from simple Langmuir Hinshelwood to more advanced micro-kinetic models based on diverse mechanistic steps. For the present study, the selected model (referred to as Eq. (1)) assumes that the adsorption of reactants is competitive and H_2 dissociates. This model is inspired from Saeys et al. [5] and Neyestanaki et al. [7]. The modeling approach and model discrimination is out of the scope of the present study and will be reported elsewhere.

The rates of formation of products *cis*- and *trans*-dimethylcyclohexane (DMCH) can be modeled by:

$$r_i = k_i \frac{K_{oX}\, p_{oX} (K_{H_2}\, p_{H_2})^{n_i}}{(1 + K_{oX}\, p_{oX} + \sqrt{K_{H_2}\, p_{H_2}})^2} \quad (1)$$

where i stands for *cis*- or *trans*-DMCH (i = 1 and 2 for *cis*- and *trans*-DMCH, respectively), k_i is the rate constant, which follows the Arrhenius law: $k_i = A_i e^{-E_i RT}$. K_{oX} is the equilibrium constant of adsorption of *o*-xylene: $K_{oX} = e^{-(\Delta H_{oX} - T\Delta S_{oX})/RT}$. K_{H_2} is the equilibrium constant of adsorption of H_2 (same notation as K_{oX}) and n_i is the H_2 partial pressure order. Parameters p_{oX} and p_{H_2} are the partial pressures of *o*-xylene and H_2, respectively

2.6. Temperature programmed oxidation

TPO experiments were performed on spent catalysts in order to study coke deposition. 50 mg of used catalyst were loaded in a quartz tubular reactor under a flow (30 mL/min) of 25% O_2–75% N_2. A temperature ramp of 15 °C/min was applied between 20 °C and 800 °C. The products, CO and CO_2 were measured by mass spectrometry. The amount of CO was always negligible.

3. Results and discussion

3.1. Deactivation studies

3.1.1. Deactivation modeling

The deactivation decay curves acquired for six representative catalysts over a period of ca. 5 h are reported in Fig. 2. As a general trend, the more active the catalysts, the fastest the initial deactivation. All catalysts deactivate exponentially in the very first hour on stream, followed by a further exponential decay (essentially for Ni-based systems) or by a linear deactivation (essentially for the noble metal-based systems). These profiles were classified into two categories which were described by a simple exponential model (Eq. (2)) or a simple linear model, such as (Eq. (3)), respectively:

$$r = r_\infty + \alpha\, e^{-t/\tau} = r_0 + \alpha(e^{-t/\tau} - 1) \quad (2)$$

$$r = r_0 - vt \quad (3)$$

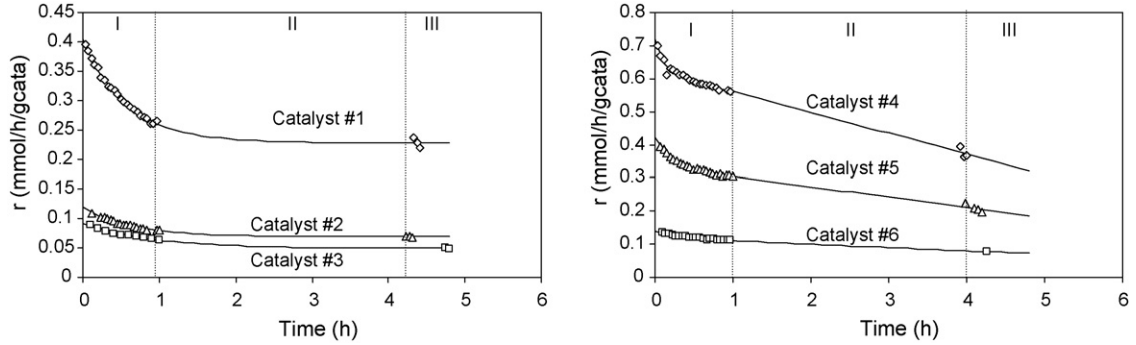

Fig. 2. Deactivation profiles during *o*-xylene hydrogenation carried out at 110 °C for six selected catalysts. (Left) Exponential decay model (Eq. (2)); (Right) Linear (Eq. (3)) decay model. Experimental steps I, II and III described in Section 2 are reported on the graphs.

where r is the activity (in mmol/(h g_{cat})), r_∞ the residual activity; α the pre-exponential factor ($r_0 = r_\infty + \alpha$) and τ the relaxation time; r_0 the initial activity; v the rate of linear decrease.

Though a precise identification of the origin of the decay processes is far beyond the scope of this study, a qualitative approach of the aging phenomena can be attempted, which might be further used for explaining the various types of observed decay profiles.

Accounting for the low temperature of the aging tests (110 °C in Fig. 2), the sintering of metal particles can be ruled out, unless a process of carbonylation, favored at low temperature, would favor a metal transfer from small to large particles via vaporization and condensation of $Ni(CO)_4$. However, the latter would imply the formation of CO via a permanent oxygen entry (system leaks), which was not detected along the experiments. Another possibility would be to consider a permanent flux of poison for the active sites, like sulfur compounds in the inlet feed. Again this hypothesis can be ruled out since this would have lead to systematic frontal poisoning, i.e., characterized by an essentially linear profile and would have affected all catalysts, which by far was not the case. The third and most likely aging process is related to carbon deposition. TPO experiments were carried out for investigating that hypothesis, as reported below.

3.2. Coke characterisation

Example of TPO profiles performed on a series of aged catalysts to characterize coke deposition are reported in Fig. 3.

Though these profiles correspond to catalysts which have been aged at different contact time (i.e., different catalyst loading), some general trends can be proposed according the nature of the systems:

(i) For the Ni-based catalyst (ex: catalyst #3), several kinds of carbon deposits are revealed. Referring to previous analyses of carbon deposits [15], the low (<200 °C) and medium (ca. 400 °C) temperature CO_2 peaks would correspond to the combustion of atomic carbon deposited on the surface of the Ni particle (surface carbide) or linked to the particles (bulk carbide or filaments), respectively. The high temperature peak (ca. 800 °C) would correspond more to highly graphitic carbon accumulating outside the metal particles.

(ii) For the noble metal-based systems (ex: catalysts #6, #7), the low and medium temperature peaks are hardly observed, as expected from poorly cracking metals, while high temperature peaks develop with time on stream. Within the frame of the *o*-xylene hydrogenation, these peaks might correspond to poly-aromatic-based carbon slowly accumulating at the entrance or within the pores of the support.

From these tentative assignments (further experiments on coke identification are in progress) and the open literature [10–12] it might thus be proposed that:

(i) the exponential-like decay (essentially observed for the Ni-based systems like the catalysts #1–3 in Fig. 2) is related to a

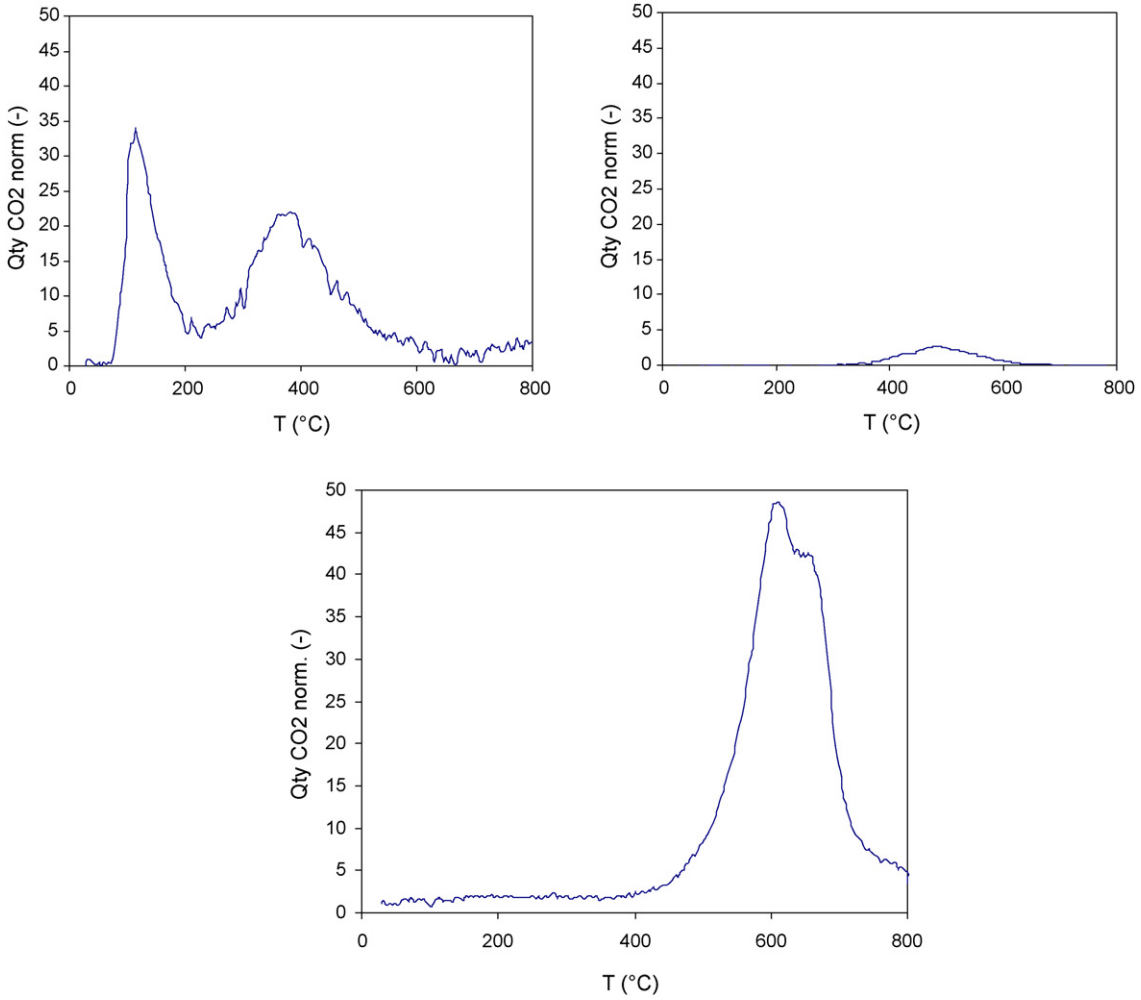

Fig. 3. TPO profiles for: (upper left) catalyst #3 (Ni/Al_2O_3); (upper right) catalyst #6 ($Pt–Sn/Al_2O_3$); (bottom) catalyst #7 (Pd/Al_2O_3).

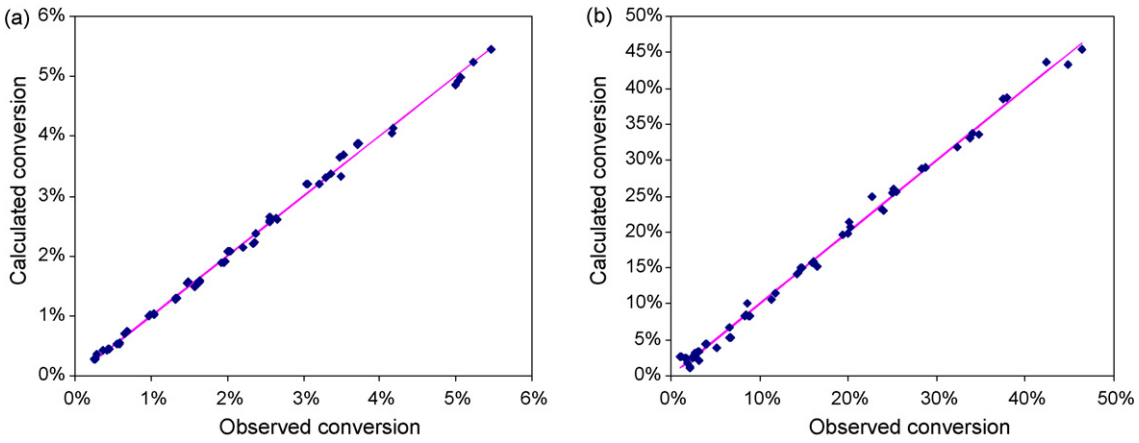

Fig. 4. Parity plots resulting from the kinetic modeling for: (a) benchmark stable catalyst #7 (Pd/Al_2O_3) and (b) catalyst #3 Ni/Al_2O_3 which deactivates by 46% in 4.8 h under testing conditions. Experimental data are not corrected against deactivation.

direct effect of carbon deposition on the intrinsic activity of the active phase (e.g., changing from metal to carbidic phase),

(ii) for the case of linear-type decay profiles essentially observed for noble-based systems, the carbon deposition would affect more transport phenomena (e.g., pore resistance or plugging due to poly-aromatic coke deposition). Indeed the combination of both effects (e.g., for long term aged Ni-based systems) cannot be excluded.

3.3. Development of a robust kinetic model

The target to develop a methodology allowing a fast access to kinetic parameters for a large number of catalysts imposes that the number of experimental conditions tested shall be limited. In so far, kinetic parameters of the catalyst library were derived from 15 to 30 data points using the kinetic model presented in Section 2.

As the model (Eq. (1)) is designed to describe the intrinsic hydrogenation kinetics, it might be assumed that deactivation impacts the quality of the fit. Indeed, one could anticipate that the more pronounced the deactivation, the larger the deviation from the model. Surprisingly, we have observed that the model enables to describe deactivating catalyst equally well, as shown in Fig. 4 for catalyst #3. As a result, the model parameters are biased by deactivation phenomena and thus do not describe accurately the intrinsic hydrogenation properties of the catalyst. The estimation of the deviation to the model from the observed data and the regression errors can hardly be estimated. In order to assess parameter estimation quality, the impact of deactivation rates on kinetic parameters was systematically investigated.

3.4. Effect of type and rates of deactivation on kinetic parameter estimation

The effect of type and rates of deactivation on kinetic parameters was investigated by simulating deactivation profiles. Both exponential and linear type deactivation profiles were applied to the kinetic data measured for catalyst #7 in order to simulate deactivating catalysts. This set of data was chosen since catalyst #7 does not deactivate under testing conditions. The normalized decays with TOS are reported in Fig. 5 and the corresponding simulated conversion values calculated for different rates of deactivation are reported in Fig. 6. These rates of deactivation correspond arbitrarily to the percentage of deactivation corresponding to the 14th h on stream in Fig. 5.

As can be seen in Fig. 6 and as expected, the higher the deactivation rate the larger the impact on the conversion level whatever the type of deactivation. In addition, the largest impacts are observed at high temperatures which were recorded at the end of the kinetic screening (end of step II). Finally, we can observe a stronger bias at low temperature (first minutes of step II) for the exponential deactivation mode than for the linear one.

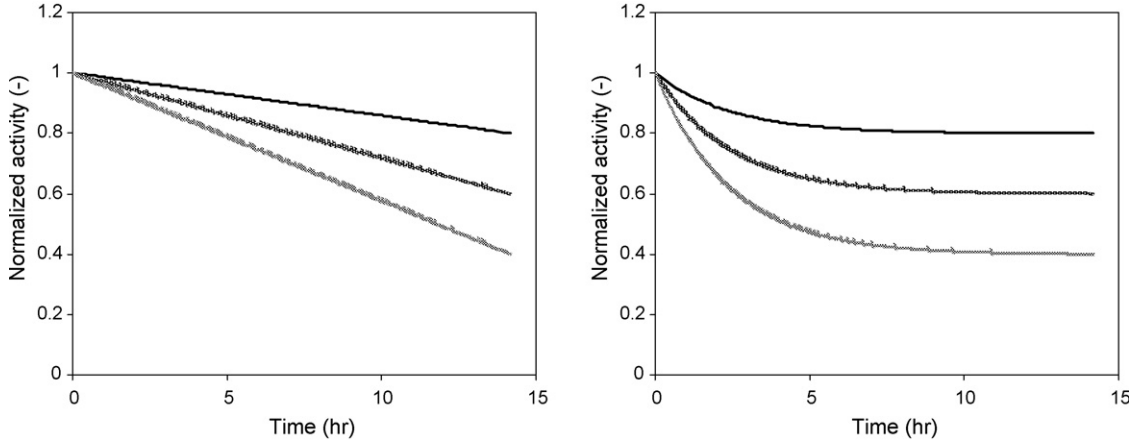

Fig. 5. Simulated deactivation profiles applied to the experimentally stable catalyst #7. (Left) linear deactivation; (right) exponential deactivation; (both) global activity loss 20% 40% 60%

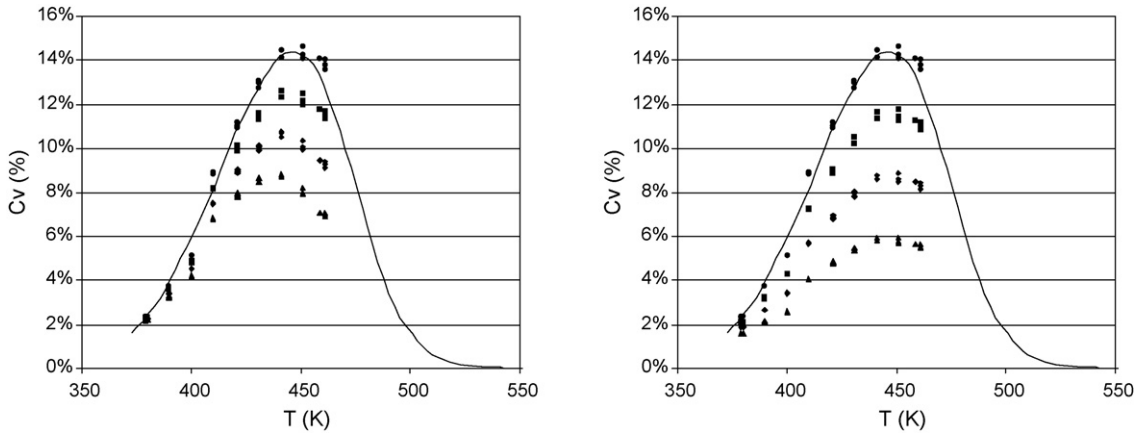

Fig. 6. Simulated conversion data when applying different profiles of deactivation. Plain lines correspond to the kinetic model. Dots represent simulated deactivated conversion data when applying different deactivation rates for linear (right) and exponential (left) profiles, respectively. Global activity loss corresponding to the simulated deactivation rates: (●) 0%, (■) 20%, (◆) 40%, (▲) 60%.

Kinetic parameters were estimated from the simulated conversion data for both linear and exponential deactivation profiles and for deactivation rates ranging from 10 to 60%. The effect of deactivation on kinetic parameters can be seen in Fig. 7 for four kinetic parameters, namely: hydrogen order for the formation of the *cis*-product *nCis*, hydrogen adsorption enthalpy $\Delta H(H_2)$ and entropy $\Delta S(H_2)$ and apparent activation energy E_1 for *cis*-DMCH formation.

As can be seen, the higher the deactivation rates, the larger the bias from the intrinsic kinetic parameters (i.e., corresponding to the absence of deactivation). The most striking effect on the kinetic parameters takes place when assuming a linear deactivation—which is the most frequent case encountered in our experimental data, and which corresponds essentially to noble metal-based systems. Here, $\Delta H(H_2)$ (hydrogen adsorption enthalpy) and *nCis* (order towards hydrogen partial pressure for the formation of *cis*-DMCH) are the parameters the most affected, i.e., decreased by deactivation. Linear deactivation tends also to decrease $\Delta H(H_2)$ and *nCis* order while E_1 (activation energy for the formation of *cis*-DMCH) and $\Delta S(H_2)$ (hydrogen adsorption

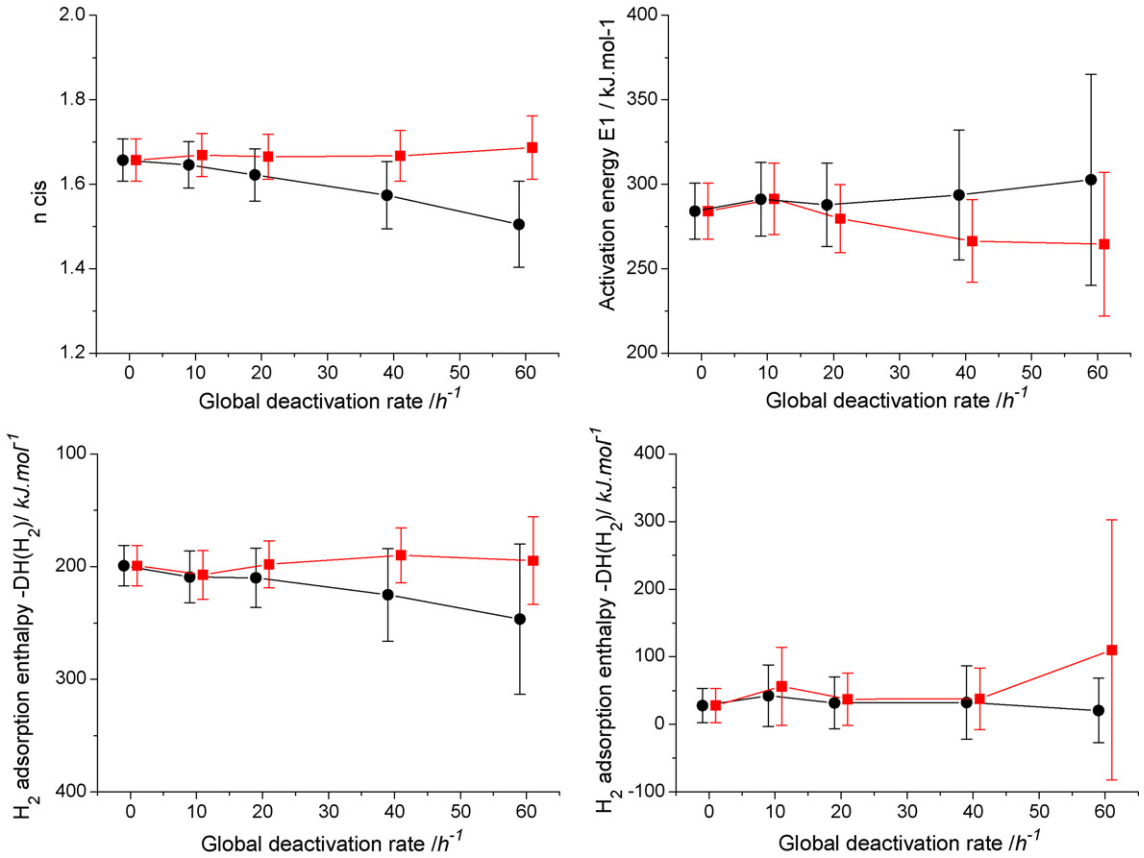

Fig. 7. Kinetic parameters for the *o*-xylene hydrogenation reaction estimated from the simulated data, as a function of deactivation rates, assuming linear (circle) and exponential (square) deactivation profiles. (Upper left) Adsorption enthalpy of hydrogen; (upper right) adsorption entropy of hydrogen; (bottom left) activation energy for the formation of *cis*-DMCH; (bottom right) order of H_2 partial pressure for the formation of the *cis*-product.

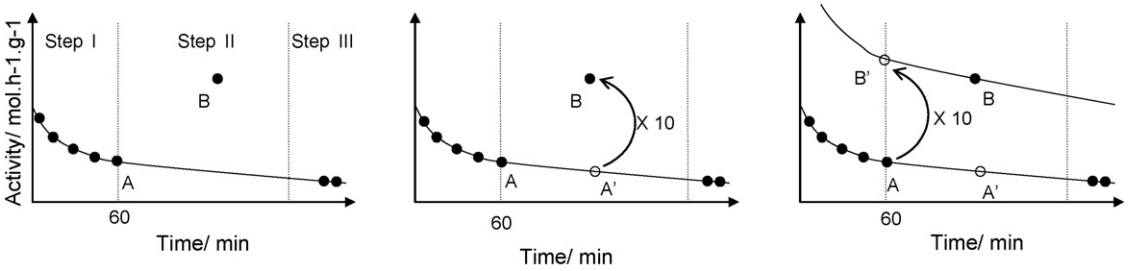

Fig. 8. Three steps process describing data correction from deactivation.

entropy) remain almost unchanged. In contrast, exponential deactivation affects essentially E_1 which decreases markedly with rate of deactivation, the other parameters being almost unchanged.

From the previously discussed origins of deactivation, tentative explanations can be proposed for the above-mentioned effects of the assumed deactivation modes, linear or exponential:

(i) The linear mode which could be assigned to pore restriction/blockage effects could hinder the diffusion of *o*-xylene onto metal particles. It could be anticipated that coke deposited onto the vicinity of metal particles limit the adsorption of *o*-xylene on the support and therefore reduce hydrocarbon spillover onto the support (we have noticed significant adsorption of xylene onto alumina supports). As a result the H_2/xylene ratio would be larger on the metal particles. Alternatively, pore restriction/blockage effects could imply a higher partial pressure of hydrogen within the partially plugged pores, i.e., around the metal active phase, due to the easier diffusion of hydrogen as compared to the reactant hydrocarbon. The direct reaction of *o*-xylene on alumina acid sites to form coke precursors would also decrease its partial pressure around the metal phase, and indirectly increase the relative pressure of hydrogen. Whatever the actual mechanism, these effects would explain the observed sensitivity for kinetic parameters directly monitored by H_2 partial pressure ($\Delta H(H_2)$ and *nCis*).

(ii) The exponential mode which could be due to a change in the reactivity of the active phase (by surface or bulk carbidization) would logically affect essentially parameters which directly reflect active surface reactivity like the apparent activation energy E_1 (electron transfer from carbon to nickel might originate the observed effect).

It can be noted finally that the confidence intervals are also affected by deactivation, tending to increase with the rate of deactivation. This can be assigned to a progressive lack of fit when simulating larger rates of deactivation.

Therefore, as already stressed in the introduction section, data must be corrected from deactivation to determine the true kinetic parameters of the hydrogenation reaction.

3.5. Method for correcting kinetic data from deactivation

In the frame of accelerated kinetic studies, a systematic evaluation of deactivation under different conditions cannot be envisaged because it would considerably slow down the screening process. Therefore, a methodology has to be implemented to correct the kinetic data recorded under various conditions (during step II of the testing sequence) from deactivation.

The basic feature of the proposed procedure is to recalculate all the kinetic data acquired during step II in order to have them corresponding to the state of the catalyst after an initial aging period of 1 h (step I).

(i) First, a regression is performed on the activity as a function of time by using deactivation models (Eq. (1) and (2)) on data acquired in steps I and III as reported above (Fig. 8, left).

(ii) Then, the ratio between one experimental activity measurement (given condition of P and T) acquired at time t during the step II kinetic screening (point B) and the extrapolated data under deactivation conditions (point A') is calculated (Fig 8, middle). Here, the example gives a ratio $rB(t)/rA'(t) = 10$.

(iii) The corrected activity data corresponding to 1 h on stream (rB') is calculated by extrapolating the observed activity at $t = 60$ min according to $rB'(60) = rA(60) \times rB(t)/rA'(t)$. In the example $rB'(60) = rA(60) \times 10$ (Fig. 8 right).

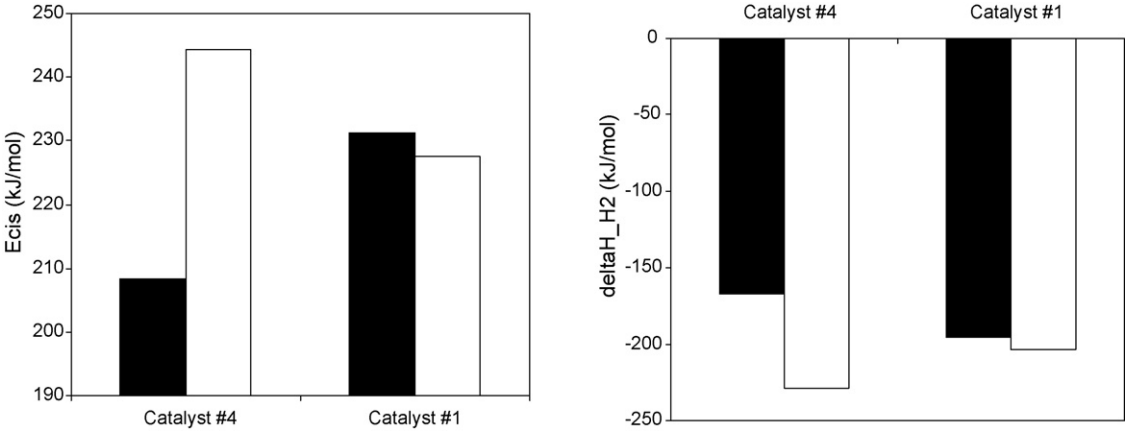

Fig. 9. Kinetics parameters for catalysts #1 and #4. (Left) Activation energy for *cis*-product formation; (right) H_2 adsorption enthalpy (Black) corrected data; (white) uncorrected data.

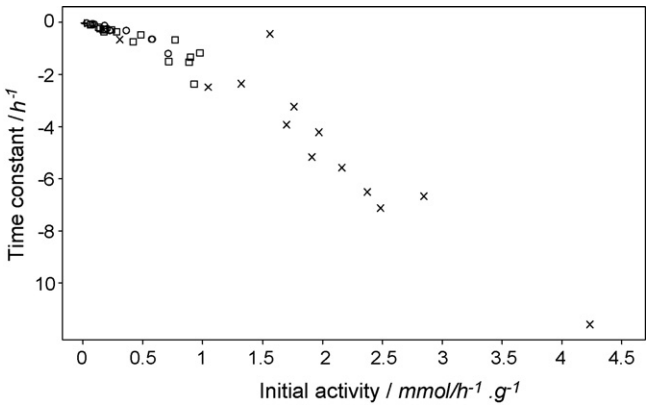

Fig. 10. Deactivation constant as a function of the initial activity (Eq. (2)) (□) Pt; (○) Ni; + Pd; (×) Rh.

The effect of data correction on the kinetic parameter estimation (Eq. (1)) was calculated for catalysts #1 & #4 as case studies (Fig. 2).

As can be seen in Fig. 9, the level of kinetic data correction depends on catalysts. The correction reduces the activation energy (E_1) of about 10% for catalyst (catalyst #4) whereas it is almost unchanged for catalyst #1. Same trends are observed for ΔH. Those results are not surprising since catalyst #1 practically does not deactivate any more after 60 min (exponential deactivation mode) whereas catalyst #4 continues to strongly deactivate after this initial period (linear deactivation mode) (Fig. 2). Thus, the correction of kinetic parameters shall be as pronounced as the deactivation is strong and continuous.

In a summary, by reprocessing the kinetic data of the reaction model according to various deactivation models, "intrinsic" kinetic parameters (ΔH, ΔS, E_a) can be calculated as true descriptors of the studied systems. Hence catalysts can be compared on a quantitative and rational basis.

3.6. Deactivation parameters as catalyst descriptors

Deactivation parameters can also be regarded as catalyst descriptors since they capture intrinsic catalytic properties. As shown in this study, deactivation after the first hour on stream was described by either exponential or linear models. Among the 44 distinct catalysts, 15 were tested twice with different contact times. We have always observed very similar deactivation patterns for same catalyst. Finally on a total of 59 deactivation experimentations, 43 can be described by linear model and 16 by exponential model. For linear behaviors, we have investigated the relationship between the initial activity and the deactivation rate (Fig. 10).

Obviously, initial activity and deactivation slope are linearly correlated. The higher the initial activity, the steeper the linear deactivation slope. We can observe highest initial activities for Rh-based catalysts although noble metal wt.% loading are equivalent for all catalysts. Based on mono-metallic catalyst characterization, we can rule out the effect of metal dispersion since we observe similar particle sizes. These results confirm theoretical calculations from Toulhoat et al. who predict Rh as the most active noble metal on volcano curves for hydrogenations of ethylene and benzene [16].

3.7. What are the catalysts features that direct deactivation modes?

Despite the tentative simplified classification between Ni-based and noble metal-based systems proposed in the previous sections, the detailed combination of catalysts features that direct the deactivation to either linear or exponential profile are not straightforward. As a matter of fact, by considering the whole studied library, it is not obvious to determine which metal, dopants and support lead significantly (i.e., with a strong statistical weight) to a given deactivation profile. In order to identify discriminating parameters of the deactivation types we have used the "classification tree" statistical method. Different algorithms were investigated and lead to similar conclusions. In this report, we present results obtained with the C&RT algorithm implemented in Statistica 6.0© (Table 2) [17]. In this data analysis, the independent variables are the synthesis parameters (two supports, four main metal, five dopants, two dopant loadings) and the dependant variable to predict is the deactivation profile (linear or exponential). Goodness-of-fit is estimated with the Gini measure.

Table 2
Classification results

	Observed cases	
	Exponential behavior	Linear behavior
Predicted cases		
Exponential behavior	11	8
Linear behavior	3	22

The algorithm provides a global prediction rate of 66%. The statistical model tends to misclassify at roughly the same rate (≈33%) predicted linear behavior in observed exponential linear and reciprocally.

The most discriminating variable is the presence/absence of Pt splitting catalysts in two groups catalysts with Pt (12 cases) and catalysts without Pt (32 cases). The latter is split again with respect to the presence of In. Indeed, considering catalysts with the following profiles Pt containing or In doped catalysts (without Pt), there is 15 chances over 16 to observe a linear deactivation. On the other hand, there is no relevant parameter which enables to predict the deactivation model with high confidence of the 28 remaining catalysts. More complex combination of parameters would discriminate more accurately the catalysts. However more data would be required to perform a proper assessment of the model.

It is worthwhile to note that exponential profiles are more frequent in the presence of Ni, as anticipated from the previous discussions. On the other hand, in addition to the composition parameters used for the above statistical analysis, other parameters might be considered as well to predict more precisely the deactivation type. These parameters could be structural variables (particle sizes and distribution, proportion of alloy for bimetallic particles, support pore size distribution, acido-basic properties, etc.) or external parameters (reactor design, isotherm or adiabatic features, etc).

4. Conclusions

HT kinetic investigation enables to obtain key quantitative information as kinetic parameters. Key kinetic parameters may be used as fine catalyst descriptors which can then be processed for QSAR studies. With this knowledge in hand, new guidelines for catalyst profiling or catalyst design can be proposed. This study addresses deactivation issues in the frame of parallel kinetic investigations. We report technologic and methodological solutions that enable to measure intrinsic kinetic parameters which describe catalyst features.

Acknowledgments

We thank the European Union for financial support and TOPCOMBI project (no. 515792).

References

[1] A.K. Neyestanaki, P. Maki-Arvela, H. Backman, H. Karhu, T. Salmi, J. Vayrynen, D.Y. Murzin, J. Mol. Catal. A-Chem. 193 (2003) 237.
[2] S. Smeds, D. Murzin, T. Salmi, Appl. Catal. A150 (1997) 115.
[3] M.V. Rahaman, M.A. Vannice, J. Catal. 127 (1991) 267.
[4] H. Backman, A.K. Neyestanaki, D.Y. Murzin, J. Catal. 233 (2005) 109.
[5] M. Saeys, M.-F. Reyniers, J.W. Thybaut, M. Neurock, G.B. Marin, J. Catal. 236 (2005) 129.
[6] M.A. Keane, J. Catal. 166 (1997) 347.
[7] A.K. Neyestanaki, P. Maki-Arvela, H. Backman, H. Karhu, T. Salmi, J. Vayrynen, D.Y. Murzin, J. Catal. 218 (2003) 267.
[8] R. Melendrez, A. Alarcon, G. Del Angel, R. Gomez, React. Kinet. Catal. Lett. 70 (2000) 113.
[9] W. Huybrechts, J. Mijoin, P.A. Jacobs, J.A. Martens, Appl. Catal. A243 (2003) 1.
[10] J.J. Birtill, Ind. Eng. Chem. Res. 46 (2007) 2392.
[11] J.J. Birtill, Catal. Today 81 (2003) 531.
[12] M. Guisnet, V. Fouche, M. Belloum, J.P. Bournonville, C. Travers, Appl. Catal. 71 (1991) 295.
[13] G. Morra, A. Desmartin-Chomel, C. Daniel, U. Ravon, D. Farrusseng, R. Cowan, M. Krusche, C. Mirodatos, Chem. Eng. J. 138 (2008) 379.
[14] AMTEC GmbH, www.amtec-chemnitz.de.
[15] L. Pinaeva, Y. Schuurmann, C. Mirodatos, in: M. Merceds Maroto-Valer, Chunsan Song, Yee Soong (Eds.), Environmental challenges and greenhouse gas control for fossil fuel utilization in the 21st century, 2002, p. 313.
[16] H. Toulhoat, P. Raybaud, J. Catal. 216 (2003) 63.
[17] L. Breiman, J.H. Freidman, R.A. Olshen, C.J. Stone, Classification and regression trees, Wadsworth International Group, Belmont, Calif, 1984, , ISBN: 0534980546.